

Activated Carbon as an Adsorbent for CO₂ Capture: Adsorption, Kinetics, and RSM Modeling

Hedi Jedli,* Maha Almonnef, Raja Rabhi, Mohamed Mbarek, Jbara Abdessalem, and Khalifa Slimi



Cite This: ACS Omega 2024, 9, 2080–2087



Read Online

ACCESS |

Metrics & More

Article Recommendations

ABSTRACT: The main objective of this research is to investigate the adsorption isotherms and the optimization of the carbon dioxide (CO₂) adsorption process on activated carbon (AC). The AC has been characterized by X-ray diffraction, scanning electron microscopy, and nitrogen (N₂) adsorption–desorption. The CO₂ isotherms measured under three adsorption temperatures (318, 308, and 298 K) were investigated by the Langmuir and linear driving force model. It is found that the Langmuir model could well predict the adsorption behavior of AC with a correlation factor of about 0.99. The kinetic model shows that the amount of CO₂ increases at higher pressures. The response surface methodology (RSM) was applied to investigate the effects of process variables and their interaction on the response to reach the optimal conditions. Based on the analysis of variance, pressure and temperature are the main factors influencing the CO₂ adsorption capacity. The effective parameters obtained through this model are found to have a value of $p < 0.05$. In addition, a semiempirical correlation was developed under the optimal operating conditions which are 25 °C and 9 bar. The results indicated that RSM models provide an effective method for evaluating CO₂ adsorption. These results point that AC is a potential adsorbent for CO₂ capture.

1. INTRODUCTION

Carbon dioxide rejected into the atmosphere by human activities is considered the main cause of global warming.¹ Many strategies have been used to reduce carbon dioxide in the environment, mainly carbon capture and sequestration.² Adsorption is the most used technique for gas separation among other techniques such as the absorption, membranes, and cryogenics.³ Therefore, the development of an adsorbent with high adsorption efficiency is crucial for a good adsorption performance.⁴ Some adsorbents have been developed for CO₂ adsorption including zeolite, metal oxides, meso porous silica, and activated carbon (AC).⁵ Among these adsorbents, AC is classified as an effective adsorbing material in the gas treatment process owing to its greater adsorption ability and low cost.⁶ In recent years, the kinetics and adsorption isotherms have been crucial factors to evaluate the performance of gas storage, separation, or purification systems based on the adsorption process. For these, Mehra and Paul et al. (2022)⁷ studied the CO₂ adsorption on five carbon nanomaterials. Mashhadimollem et al. (2021)⁸ measured and modeled the CO₂ adsorption on different biomass with artificial neural networks. Gautam and Sahoo (2022)⁹ compared various ACs as adsorbents to capture CO₂ from ambient air. Zhang et al. (2010)¹⁰ analyzed the CO₂ adsorption kinetics on AC at different pressures and temperatures with the linear driving force (LDF) model. Balsamo et al.¹¹ investigated the dynamic of CO₂ adsorption onto AC. Jribi et al. (2017)¹² studied the CO₂ adsorption kinetics on AC with the modified LDF equation. Liu et al. (2012)¹³ found that the adsorption kinetics of CO₂ on amine-functionalized carbon nano tubes are governed by intra particle diffusion. Teng et al. (2017)¹⁴ observed that CO₂ adsorption on MCM-41 is influenced by both in-film diffusion and intra

particle diffusion. Khajeh and Ghaemi et al. (2020)¹⁵ worked CO₂ adsorption by nano clay montmorillonite and found that CO₂ capacity was 100.67 mg/g. Khoshraftar and Ghaemi et al. (2022)¹⁶ investigated the CO₂ adsorption on AC produced from pistachio shells and modeled the adsorption isotherms with the neural network (ANN). As seen previously, different parameters such as adsorption capacity, pressure, and temperature can affect the adsorption mechanism. In addition, the impact of these variables was investigated as being independent or constant. To remove the limits and flaws of the present methods, it is important to enhance the effective elements with response surface methodology (RSM).

In this paper, AC prepared from olive waste was used as an adsorbent for carbon dioxide capture. Various methods such as X-ray diffraction (XRD), scanning electron microscopy (SEM), and Brunauer–Emmett–Teller (BET) have been used to identify the properties of the AC. A regression equation model was constructed and then optimized using the RSM. The RSM was used to evaluate the effect of CO₂ adsorption capacity as the response function, based on temperature and pressure as independent variables. The adsorption experiments provided by Langmuir isotherm data and kinetic curves were investigated.

Received: April 20, 2023

Revised: December 14, 2023

Accepted: December 19, 2023

Published: December 29, 2023



2. ADSORBENT CHARACTERIZATION

Olive waste is an agricultural residue produced mainly in the Mediterranean countries such as Tunisia, which is one of the main producers of olive oil (Figure 1).¹⁷



Figure 1. Tunisian olive waste.

This waste causes many environmental problems to countries producing olive oil, and this is a good way to increase its value by recycling it. Due to its availability and cost, this material is widely used in the production of AC.¹⁷

The AC used in this work is prepared from olive wastes with chemical modifications.¹⁶ The CO₂ adsorption was measured at different temperatures with a Nova 4200e static volumetric analyzer (Quantachrome). The functional groups of the sample were characterized by FTIR spectrometer Vertex 7. The morphologies were examined on a Thermo Fisher FEI Q250 scanning electron microscope. XRD patterns were conducted with a Philips MPD1880-PW1710 diffractometer. N₂ adsorption–desorption isotherm was made with a Micromeritics 3-Flex. BET analyses were predicted to determine the surface and the pore sizes.

3. ADSORPTION MODEL

The experimental adsorption isotherm was modeled by the Langmuir model. This model was considered the most suitable for monolayer adsorption and for depiction of the homogeneous surfaces. It is employed for the chemical and physical adsorptions and is one of the most popular methods for implicit adsorption. It is given by the following equation¹⁶

$$q = q_m \frac{K_L p}{1 + K_L p} \quad (1)$$

where q_m , q , K_L and p present the CO₂ maximum capacity (cm³/g), the CO₂ adsorbed amount (cm³/g), the Langmuir constant, and the equilibrium pressure (bar).

The validity of the adsorption isotherms is confirmed by the value of the correlation coefficient (R^2) and the normalized standard deviation (ΔQ), which is established as following equation¹⁸

$$\Delta Q (\%) = \sqrt{\frac{\sum_i^n (Q_{\text{exp}} - Q_{\text{cal}}/Q_{\text{exp}})^2}{n}} \times 100 \quad (2)$$

where Q_{exp} means the experimental adsorbed quantity, Q_{cal} is the calculated adsorbed amount, and n is the data point number of the adsorption isotherm.

4. KINETICS MODEL

Many models are used to describe the adsorption kinetics of different gases on various adsorbents. The first model that takes into account adsorption rate as a function of adsorption capacity is the pseudo-first-order equation suggested by Lagergreen.¹⁹ Nevertheless, the most used model to depict the adsorption rate of CO₂ was the LDF model. This model is expressed by the following equation¹⁸

$$\frac{\partial q}{\partial t} = k_{\text{eff}}(q^* - q) \quad (3)$$

The integral equation was written as following

$$\ln\left(\frac{q^* - q}{q^*}\right) = -k_{\text{eff}}t \quad (4)$$

where q presents the CO₂ amount at time t , q^* is the CO₂ amount adsorbed at the equilibrium, and k_{eff} was the mass-transfer constant.

The activation energy (E_a) is determined using the Arrhenius formula¹⁹

$$k_{\text{eff}} = A \exp\left(-\frac{E_a}{RT}\right) \quad (5)$$

This equation can be express in the following¹⁸

$$\ln k_{\text{eff}} = \ln A - \frac{E_a}{RT} \quad (6)$$

where E_a represents the Arrhenius factor, A is the Arrhenius activation energy, and R is the gas constant.

5. RESPONSE SURFACE METHODOLOGY

In the past few years, the RSM was widely used by the scientists. The RSM is designed to optimize the response variable through a mixture of statistical and mathematical approaches. This approach is used to analyze and model problems where the response variable can be influenced by different independent variables.²⁰ The response parameters are estimated within a defined range.²¹ In the RSM optimization, the input variables are determined as an independent variable. Eq 7 yields the dependence of a response which is stated in terms of the response (Y), the input variables (X), and the error function (ϵ).¹⁵

$$Y = f(X_1, X_2, \dots, X_k) + \epsilon \quad (7)$$

The aim of the RSM design was to analyze and identify the factors influencing the output with minimum experiences conducted. The variables used in the RSM are listed in Table 1.

A complete representation of the absorption mechanism needs to be modeled as a quadratic or higher order polynomial function. Equation 8 defines the second-order model.¹⁵

Table 1. Range and Level of the Experimental Parameters

independent variables	-1	0	+1
P (bar)	1	5	9
T (°C)	25	35	55

$$y = a_0 + \sum_{i=1}^n a_i x_i + \sum_{i=1}^n a_{ii} x_i^2 + \sum_i \sum_j a_{ij} x_i x_{ji < j} + \epsilon \quad (8)$$

where y , a_0 , and ϵ were the response, the constant numeral, and the model error, respectively. X_i and X_j represent the design variables i , namely, temperature and pressure. α_p , α_{ip} , and α_{ij} are the adjustment parameters. Moreover, the variable range has been defined by the initial tests, and the data have been evaluated by analysis of variance (ANOVA). The statistical meaning is investigated with the F -value and p -value. The F -value demonstrates the highest credibility of the model that is derived with eqs 9–11.¹⁵

$$F_0 = \frac{MS_R}{MS_E} \quad (9)$$

$$MS_R = \frac{SS_R}{P - 1} \quad (10)$$

$$MS_E = \frac{SS_E}{n - P'} \quad (11)$$

where SS_R and SS_E represent the sum of squares of regression and the errors, respectively, and their expression as follows¹⁵

$$SS_R = \sum (\hat{Y}_i - \bar{Y}_i)^2 \quad (12)$$

$$SS_E = \sum (Y_i - \hat{Y}_i)^2 \quad (13)$$

Based on the regression model, we can obtain the response value (Y_i) and the mean of the responses (\bar{Y}_i).

We noticed that the model becomes significant from the p value, which must be lower than that of which in our case is 0.05. In addition, the p -value and F -value for each variable denote their effects on the model. Table 1 illustrates the levels and range of the independent variables.

6. RESULTS AND DISCUSSION

6.1. Material Characterization. The crystal phase of the AC was confirmed by XRD (Figure 2) and shows two peaks at $2\theta = 25$ and 42° . These peaks are assigned to the (002) and (100) which appear as the disordered carbon sheet. Moreover, the strong diffraction peaks revealed that the AC was amorphous.¹⁶

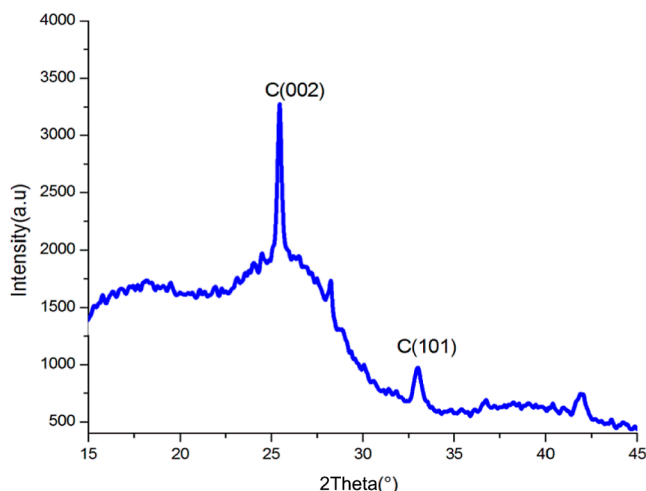


Figure 2. XRD pattern of the AC.

Figure 3 shows the morphology of the AC. As shown in the SEM image, the material surface is heterogeneous and contains

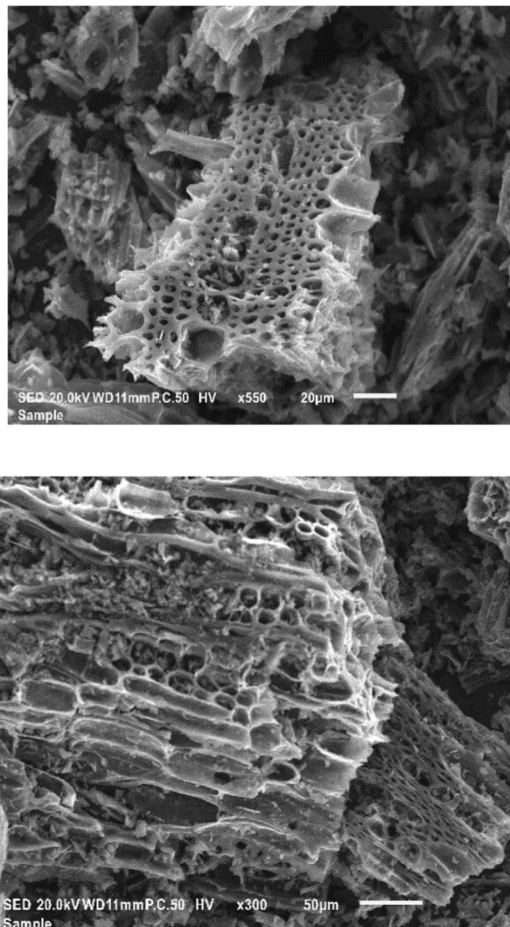
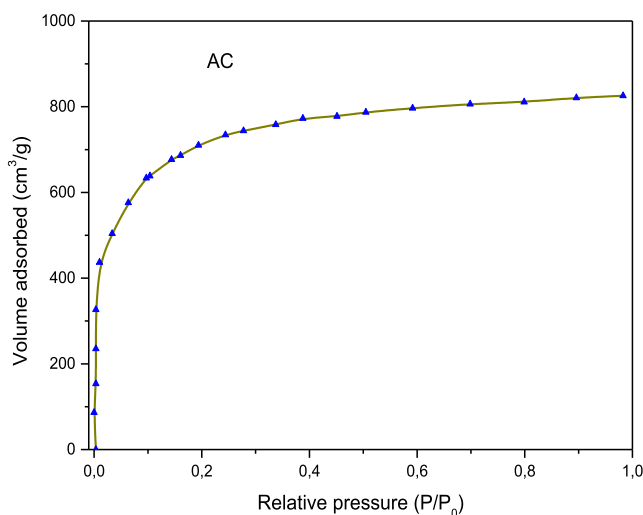


Figure 3. SEM analysis of the AC.

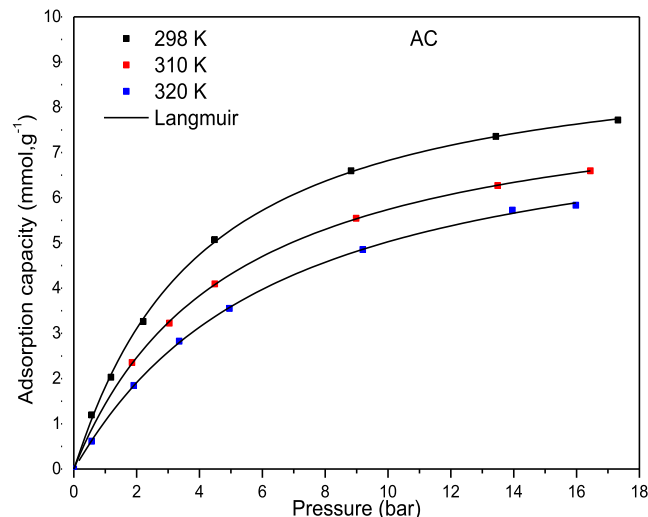
a large number of randomly distributed pores. This structure provides an efficient adsorption process since it contains free spaces suitable for the adsorbents.

The N_2 isotherms and textural parameters of AC are displayed in Figure 4 and Table 2. The N_2 isotherm shows that the AC is classed as a type I isotherm,¹⁶ and based on the IUPAC classification, the adsorbent is a microporous structure. The N_2 adsorption occurs at low pressure and then increases slightly until reaching a horizontal plateau. This phenomenon is due to the beginning of the adsorption process, there are several empty sites able to adsorb the gases. Then, there is a saturation following the filling of the sites by the molecules.

6.2. Adsorption Isotherms. The CO_2 isotherms measured at 298, 308, and 318 K are displayed in Figure 5. According to this figure, the adsorption capacity rises with the rise of the pressure. On the other hand, an increase in the temperature leads to a reduction in the CO_2 adsorbed, which points to an exothermic process.¹⁸ In fact, the binding forces between the adsorbate and the adsorbent decrease with the increase of the temperature, leading to decline on the adsorption capacity.¹⁸ The experimental data were fitted with the Langmuir model. The marker points indicate the experimental results, while the solid line gives the isotherm models. Figure 5 reveals that the Langmuir model exhibits good agreement with the experimental isotherms, with R^2

Figure 4. N_2 adsorption–desorption isotherms of the AC.**Table 2. Textural Parameters of Activated Carbon**

S_{BET} (m^2/g)	V_{mic} (cm^3/g)	V_{mes} (cm^3/g)	V_{total} (cm^3/g)
1565	0.649	0.027	0.676

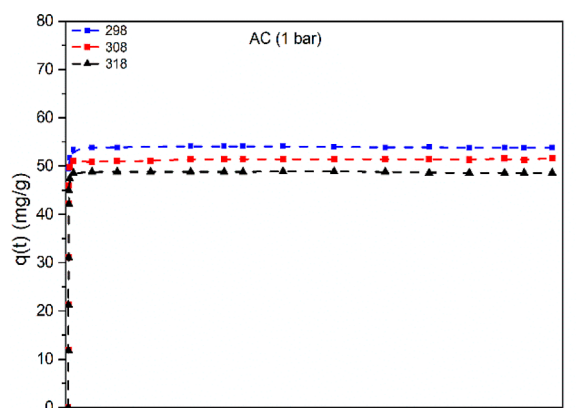
Figure 5. CO_2 adsorption isotherms on the AC.

greater than 0.98. This result suggests that the AC surface is heterogeneous.¹⁹ With regard to the Langmuir fit, it is clear from Table 3 that q_m and k values decline with increasing temperature, confirming the exothermic adsorption process.²⁰

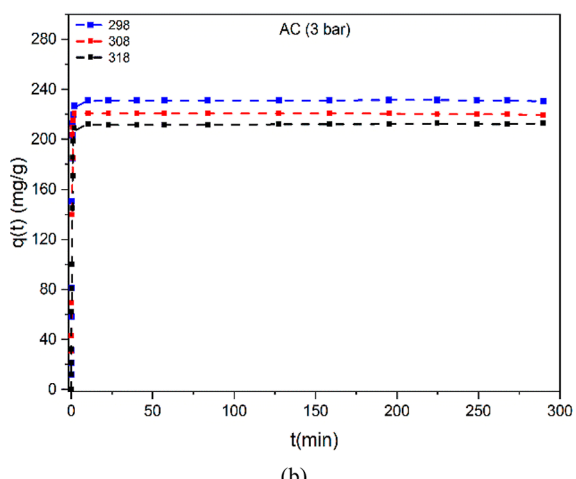
6.3. CO_2 Adsorption Kinetics. The CO_2 kinetic adsorption on the AC with different pressures and temperatures is presented in Figure 6. Following the kinetic curve, we noticed that the amount of CO_2 adsorbed on AC increased

Table 3. Parameters of the Langmuir Model

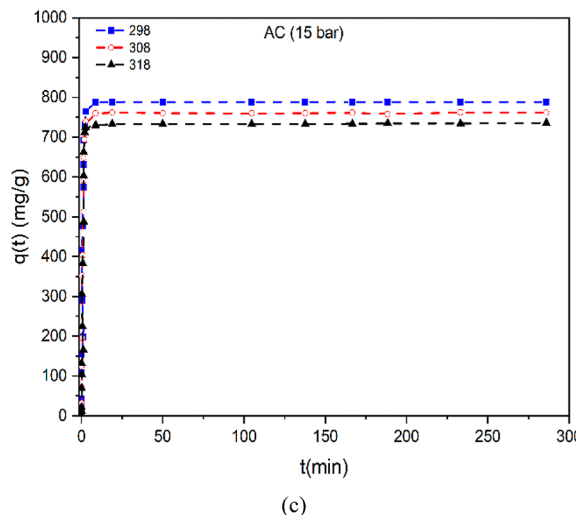
adsorbent	temperatures [K]	parameters of Langmuir model		
		q_m	K_L	R
AC	298	9.374	0.24	0.998
	310	8.571	0.20	0.994
	320	8.127	0.15	0.990



(a)



(b)



(c)

Figure 6. Adsorption kinetics curves of CO_2 on the AC at 1 (a), 3 (b), and 15 bar (c).

rapidly until reaching equilibrium. Additionally, it can be remarked that the amount of CO_2 rises at higher pressure.

The plot of $\ln\left(\frac{q^* - q}{q^*}\right)$ as a function of time (Figure 7) indicates a linear function with a correlation coefficient of 0.99. Through the slopes of these lines, we can obtain the mass-

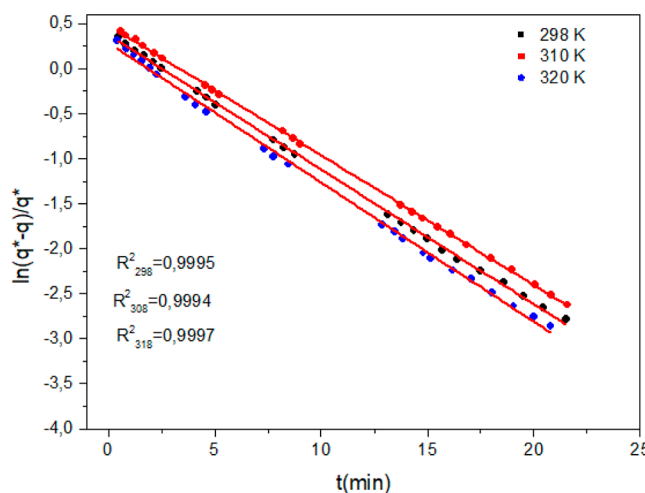


Figure 7. Linear dependence between $\ln\left[\frac{q^* - q}{q^*}\right]$ and time on the AC.

transfer coefficients of the CO₂ diffusion. The mass transfer and standard deviation are found in **Table 4**.

Table 4. Mass-Transfer Coefficients on the AC

pressure [bar]	mass-transfer coefficient	
	temperatures [K]	AC
1	298	0.0351
	310	0.0278
	320	0.0318
3	298	0.1158
	310	0.0714
	320	0.0856
15	298	0.0642
	310	0.0547
	320	0.0597

Following these values, we can see that the mass transfer rises with temperature. The CO₂ diffusion is most rapid with an increase of temperature, which allows for higher mass transfer. In addition, the mass-transfer coefficient gets higher with an increase in pressure. The plot of ln_{k_{eff}} versus (1/T) is illustrated in **Figure 8**. The plots were linearly adjusted with a coefficient (R²) of 0.99, which indicates good linearity between ln_{k_{eff}} and 1/T. Based on the E_a values (**Table 5**), we can show that E_a decreases with the increase of the pressure, which suggests that the interaction between CO₂ and the AC occurs at high pressure.^{11,20}

Following the heterogeneity of the material surface, the CO₂ is adsorbed on the adsorption sites with high-energy barriers at low pressure.²⁰ On the other hand, at high pressure, the adsorption is taken on sites present on a low-energy barrier.

6.4. RSM Analysis. **6.4.1. Analysis of Variance.** The effect of pressure and temperature, which are the principal agents of CO₂ adsorption in montmorillonite (MMT), was investigated by CCD.²¹ In addition, we consider that CO₂ adsorption capacity is the response, 13 experiments were selected to simulate the RSM model, and the order of testing was arranged randomly (**Table 6**). Depending on pressure and temperature, the adsorption capacity ranges from 3 to 105 mg of CO₂/g of the adsorbent.

To provide an effective response, the statistical validity of the model was estimated by ANOVA. The findings of these

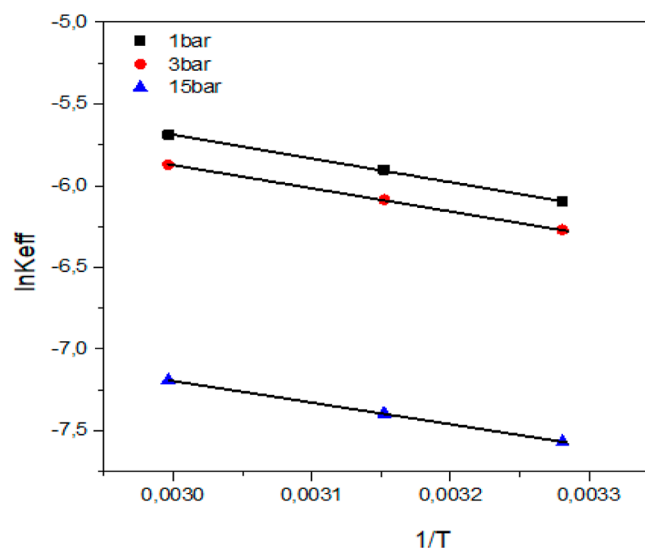


Figure 8. ln_{k_{eff}} and 1/T on the AC.

Table 5. E_a for the AC

AC	E _a [kJ/mol]		
	1 bar	3 bar	15 bar
	5.154	3.928	2.654

Table 6. Experimental Values of Design and Response of the Experiment

run	Std	X ₁ (T) (°C)	X ₂ (P) (bar)	Q (mg/g)
1	8	50	1	5.021
2	3	30	9	34.8
3	13	50	5	44.45
4	7	20	1	105.6
5	6	78	5	35.24
6	4	70	9	34.26
7	9	50	5	15.85
8	4	70	5	35.41
9	11	50	5	55.20
10	10	50	1	3
11	12	50	5	35.11
12	5	21	5	15.63
13	1	30	9	66.74

analyses were assessed using statistical parameters like F-value, p-value, and degree of freedom (df), which are listed in **Table 4**. From this table, we can see that the effective parameters obtained through this model are found to have a value of *p* < 0.05. In addition, the relevance of the model has been assessed with a correlation coefficient (R²) and the adjusted coefficients of R_{adj}². However, the smaller the *p*-value, the larger the F-value, which reveals the importance of this model. In addition, *p*-values less than 0.04 reflect the statistical fit of the model.²² For the adsorption capacity listed in **Table 7**, the *p*-value must be less than 0.0001, against 67.08 of the F-value, which points to the suitability of the quadratic model.

The regression model gives the adsorption capacity responses. This model, which is expressed by the pressure (X₁) and temperature (X₂) parameters, is written as eq 14

Table 7. ANOVA Results for the RSM-CCD Model

source	sum of squares	degree of freedom	mean squares	F-value	p-value
model	60.16	5	11.65	67.02	<0.001
X_1	9.89	1	9.81	56.15	0.001
X_2	50.6	1	50.46	284.84	<0.001
$X_1 X_2$	0.0974	1	0.0785	0.5014	0.4523
X_1^2	0.0084	1	0.0067	0.0048	0.8523
X_2^2	0.0410	1	0.0421	0.214	0.6214
residual	1.28	7	0.17458		
$R^2 = 0.998$			$R_{\text{adj}}^2 = 0.994$		

$$\begin{aligned} \text{Sqrt}(q) = & 4.0213 - 0.032103X_1 + 0.812046X_2 \\ & - 0.001807X_1X_2 - 0.0000121X_1^2 - 0.006513X_2^2 \end{aligned} \quad (14)$$

The relation of the predicted values and the experimental of the adsorption capacity is given in Figure 9. The test results are

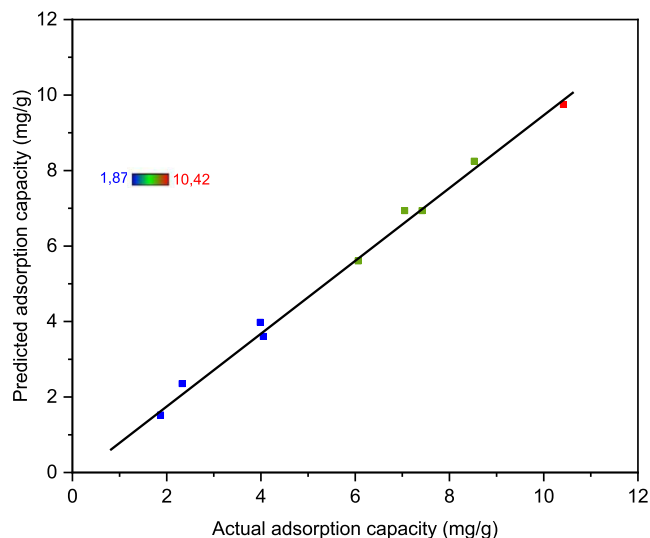


Figure 9. Actual adsorption capacity vs predicted adsorption capacity.

the measured response values, while the expected values have been determined by the assumed models. R^2 correlation values (0.998) between experimental values and calculated results indicate high reliability in this mode. These results suggest that this model is suitable to predict the experimental data and may be applied in MMT analysis in CO_2 adsorption.

6.4.2. Effects of Model Parameters. To optimize the conditions of the reaction system, it is necessary to make the graphic depictions of the regression equation in the form of 3D plot and 2D contour.²³ Figure 10 shows the interaction results between the pressure and temperature and their impact on adsorption ability. Following this figure, we can see that the pressure is an important parameter on the adsorption capacity. Figure 10a shows that higher pressure presents a favorable effect on the absorption mechanism. The pressure effect depends on the structure of the adsorbent since it is a porous structure with a specific surface area of 1565 (m^2/g) and a total volume of 0.676 (cm^3/g). Therefore, this porous structure of varying sizes affected the performance of the pressure adsorbent.

Additionally, the temperature is another effective parameter in the adsorption capacity. It can be observed that raising the temperature (Figure 10b) has a negative influence on the

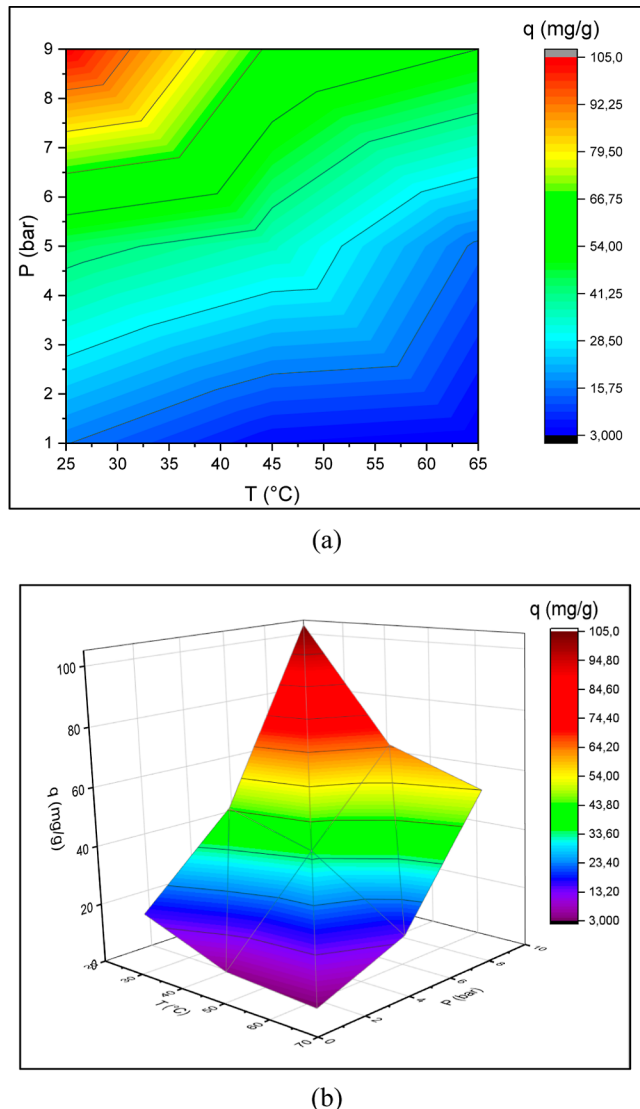


Figure 10. Response surface diagrams of the interaction of T and P : (a) 3D surface graph and (b) contour graph for adsorption capacity.

adsorption capacity. The decrease in adsorption capacity with temperature suggests the exothermic nature of the adsorption mechanism.

6.5. Comparison with Other AC. This investigation provides a comparison of the CO_2 adsorption capacity of AC prepared from olive waste with the literature. As listed in Table 8, different ACs from various CO_2 adsorption sites exhibit maximum adsorption capacities (1.85 mmol/g). As shown in this table, the AC has a similar or much higher adsorption

Table 8. Analyze the CO₂ Adsorption by Several Activated Carbon

adsorbent	T (°C)	adsorption capacity (mmol g ⁻¹)	references
pistachio shell	25	1.23	16
sugar cane bagasse	25	1.61	24
palm kernel shell	25	1.88	25
waste plastic	30	1.31	26
Norit SX2 (peat)	25	1.88	27
coconut AC	25	1.79	28
this study	25	1.85	

capacity than other types of AC such as sugar cane bagasse, palm kernel shell, waste plastic, and pistachio shell.

In fact, the AC used was developed from olive waste. This waste causes many environmental problems in oil-producing countries, and this is a good way to increase its value by recycling it.

7. CONCLUSIONS

The main objective of this research is to investigate the adsorption isotherms and the optimization of the CO₂ adsorption process on the AC. The AC was analyzed by N₂ adsorption–desorption, XRD, and SEM. The CO₂ adsorption isotherms were fitted with the Langmuir model and the linear model (LDF). The results show that at given pressure, the mass-transfer coefficient increased with adsorption temperature, and the adsorption characteristics were physical process. In addition, the effects of the operating parameters including the pressure and the temperature on the CO₂ adsorption by RSM were investigated, and the results were used to assess the impact of these parameters on the response to attain the optimum conditions. According to the ANOVA, the temperature and the pressure are the main variables which affect the CO₂ ability. The findings show that an elevated temperature has a negative influence on CO₂ adsorption, whereas an increase in pressure has a positive impact on the adsorption process. The effective parameters obtained through this model are found to have a value of $p < 0.05$. In addition, a semiempirical correlation was developed under the optimal operating conditions which are 25 °C and 9 bar. According to these results, the olive waste was an important candidate for CO₂ adsorption since it is readily available and relatively cheap. Moreover, these results are useful for separating CO₂ from gas by an adsorption technique and also for the development of a device with an adsorption process.

■ AUTHOR INFORMATION

Corresponding Author

Hedi Jedli — University of Monastir, National Engineering School of Monastir, Laboratory of Studies of Thermal Systems and Energy, Monastir 5019, Tunisia;  orcid.org/0000-0002-7862-9875; Email: jedli.hedi@gmail.com

Authors

Maha Almonnef — Physics Department, Faculty of Science, Princess Nourah Bint Abdulrahman University, Riyadh 11671, Saudi Arabia

Raja Rabhi — Department of Physics, Faculty of Science, Al-Baha University, Alaqiq 65779-7738, Saudi Arabia

Mohamed Mbarek — Research Laboratory: Assymmetric Synthesis and Molecular Engineering of Materials for Organic

Electronic (LR18ES19), Monastir University—Tunisia, Monastir 5000, Tunisia

Jbara Abdessalem — University of Sousse, Higher Institute of Transportation and Logistics, Sousse 4023, Tunisia

Khalifa Slimi — University of Monastir, National Engineering School of Monastir, Laboratory of Studies of Thermal Systems and Energy, Monastir 5019, Tunisia

Complete contact information is available at:
<https://pubs.acs.org/10.1021/acsomega.3c02476>

Notes

The authors declare no competing financial interest.

■ ACKNOWLEDGMENTS

This research was funded by Princess Nourah bint Abdulrahman University Researchers Supporting Project number (PNURSP2023R56), Princess Nourah bint Abdulrahman University, Riyadh, Saudi Arabia.

■ REFERENCES

- (1) Yang, H.; Xu, Z.; Fan, M.; Gupta, R.; Slimane, R.; Bland, A. E.; Wright, I. Progress in carbon dioxide separation and capture: a review. *J. Environ. Sci.* **2008**, *20*, 14–27.
- (2) Stewart, C.; Hessami, M. A.; Mir-Akbar, H. A study of methods of carbon dioxide capture and sequestration—the sustainability of a photosynthetic bioreactor approach. *Energy Convers. Manage.* **2005**, *46*, 403–420.
- (3) Yong, Z.; Mata, V.; Alirio, R. Adsorption of carbon dioxide at high temperature-A review, *Sep. Purif. Technol.* **2002**, *26*, 195–203.
- (4) Saha, B. B.; Koyama, S.; El-Sharkawy, I. I.; Habib, K.; Srinivasan, K.; Dutta, P. Evaluation of Adsorption Parameters and Heats of Adsorption through Desorption Measurements. *J. Chem. Eng. Data* **2007**, *52*, 2419–2424.
- (5) Yates, M.; Blanco, J.; Avila, P.; Martin, M. Honeycomb monoliths of activated carbons for effluent gas purification. *Microporous Mesoporous Mater.* **2000**, *37*, 201–208.
- (6) Sircar, S.; Golden, T.; Rao, M. Activated carbon for gas separation and storage. *Carbon* **1996**, *34*, 1–12.
- (7) Mehra, P.; Paul, A. Decoding Carbon-Based Materials' Properties for High CO₂ Capture and Selectivity. *ACS Omega* **2022**, *7*, 34538–34546.
- (8) Mashhadimoslem, H.; Vafeinia, M.; Safarzadeh, M.; Ghaemi, A.; Fathalian, F.; Maleki, A. Development of Predictive Models for Activated Carbon Synthesis from Different Biomass for CO₂ Adsorption Using Artificial Neural Networks. *Ind. Eng. Chem. Res.* **2021**, *60*, 13950–13966.
- (9) Gautam; Sahoo, S. Experimental investigation on different activated carbons as adsorbents for CO₂ capture. *Therm. Sci. Eng. Prog.* **2022**, *33*, 101339.
- (10) Zhang, Z.; Zhang, W.; Xiao, C.; Qibin, X.; Zhong, Li. Adsorption of CO₂ on Zeolite 13X and Activated Carbon with Higher Surface Area. *Sep. Sci. Technol.* **2010**, *45*, 710.
- (11) Balsamo, M.; Budinova, T.; Erto, A.; Lancia, A.; Petrova, B.; Petrov, N.; Tsyntsarski, B. CO₂ adsorption onto synthetic activated carbon: Kinetic, thermodynamic and regeneration studies. *Sep. Purif. Technol.* **2013**, *116*, 214–221.
- (12) Jribi, S.; Miyazaki, T.; Saha, B. B.; Pal, A.; Younes, M. M.; Koyama, S.; Maalej, A. Equilibrium and kinetics of CO₂ adsorption onto activated carbon. *Int. J. Heat Mass Transfer* **2017**, *108*, 1941–1946.
- (13) Liu, Q.; Shi, J.; Zheng, S.; Tao, M.; He, Y.; Shi, Y. Kinetics studies of CO₂ adsorption/desorption on amine-functionalized multiwalled carbon nanotubes. *Ind. Eng. Chem. Res.* **2014**, *53*, 11677–11683.

- (14) Teng, Y.; Liu, Z.; Xu, G.; Zhang, K. Desorption kinetics and mechanisms of CO₂ on amine-based mesoporous silica materials. *Energies* **2017**, *10*, 115.
- (15) Khajeh, M.; Ghaemi, A. Nanoclay montmorillonite as an adsorbent for CO₂ capture: Experimental and modeling. *J. Chin. Chem. Soc.* **2020**, *67*, 253–266.
- (16) Khoshraftar, Z.; Ghaemi, A. Evaluation of pistachio shells as solid wastes to produce activated carbon for CO₂ capture: Isotherm, response surface methodology (RSM) and artificial neural network (ANN) modeling. *Curr. Res. Green Sustainable Chem.* **2022**, *5*, 100342.
- (17) Abid, N.; Masmoudi, M. A.; Megdiche, M.; Barakat, A.; Ellouze, M.; Chamkha, M.; Ksibi, M.; Sayadi, S. Biochar from olive mill solid waste as an eco-friendly adsorbent for the removal of polyphenols from olive mill wastewater. *Chem. Eng. Res. Des.* **2022**, *181*, 384–398.
- (18) Almoneef, M. M.; Jedli, H.; Mbarek, M. Experimental study of CO₂ adsorption using activated carbon. *Mater. Res. Express* **2021**, *8*, 065602.
- (19) Jedli, H.; Brahmi, J.; Hedfi, H.; Mbarek, M.; Bouzgarrou, S.; Slimi, K. Adsorption kinetics and thermodynamics properties of Supercritical CO₂ on activated clay. *J. Pet. Sci. Eng.* **2018**, *166*, 476–481.
- (20) Jedli, H.; Almoneef, M.; Mbarek, M.; Jbara, A.; Slimi, K. Adsorption of CO₂ onto zeolite ZSM-5: Kinetic, equilibrium and thermodynamic studies. *Fuel* **2022**, *321*, 124097.
- (21) Krupskaya, V. V.; Zakusin, S. V.; Ekaterina, A.; Olga, D.; Anatoliy, Z.; Petr, B.; Maria, T. Experimental Study of Montmorillonite Structure and Transformation of Its Properties under Treatment with Inorganic Acid Solutions. *Minerals* **2017**, *7*, 49.
- (22) Tyagi, B.; Chudasama, C. D.; Jasra, R. V. Determination of structural modification in acid activated montmorillonite clay by FT-IR spectroscopy. *Spectrochim. Acta, Part A* **2006**, *64*, 273–278.
- (23) J Richard, E.; Carl, T. L. *Introductory Chemical Engineering Thermodynamics*; Prentice Hall PTR; Upper Saddle River, NJ, 1999; p 184.
- (24) Guo, Y.; Tan, C.; Sun, J.; Li, W.; Zhang, J.; Zhao, C. Porous activated carbons derived from waste sugarcane bagasse for CO₂ adsorption. *Chem. Eng. J.* **2020**, *381*, 122736.
- (25) Rashidi, N. A.; Suzana, Y. Potential of palm kernel shell as activated carbon precursors through single stage activation technique for carbon dioxide adsorption. Rashidi N.A., Yusup, S. *J. Cleaner Prod.* **2017**, *168*, 474–486.
- (26) Kaur, B.; Gupta, R. K.; Bhunia, H. Chemically activated nanoporous carbon adsorbents from waste plastic for CO₂ capture: Breakthrough adsorption study. *Microporous Mesoporous Mater.* **2019**, *282*, 146–158.
- (27) Rashidi, N. A.; Yusup, S.; Borhan, A. Isotherm and Thermodynamic Analysis of Carbon Dioxide on Activated Carbon. *Procedia Eng.* **2016**, *148*, 630–637.
- (28) Ali, G. A. M.; Habeeb, O. A.; Algarni, H.; Kwok Feng, C. CaO impregnated highly porous honeycomb activated carbon from agriculture waste: symmetrical supercapacitor study. *J. Mater. Sci.* **2017**, *54*, 305–320.